

Currents In Korea-Tsushima Strait During Summer 1999

H. Perkins, W. J. Teague, and G. A. Jacobs

Naval Research Laboratory, Stennis Space Center, Mississippi

K. I. Chang and M.-S. Suk

Korea Ocean Research and Development Institute, Ansan, Korea

Abstract. Results are presented from continuous current measurements across Korea-Tsushima Strait between May and October 1999. The data are from eleven bottom-mounted Acoustic Doppler Current Profilers that recorded full-depth profiles of currents along two lines, one at each end of the Strait. The two sections show markedly different mean flow regimes. At the southern entrance, the cross-section flow varies smoothly across the channel, showing a broad maximum at mid-channel. The northern section is marked by strong spatial variability but in the mean consists of two streams, one on each side of the strait. Between the two is a regime of highly variable flow with a weak mean, presumably indicating the wake from Tsushima Island. Flow variability in time is described by statistical measures and by representative snapshots.

1. Introduction

Long-term measurement from fixed instruments in Korea-Tsushima Strait (hereafter called the Strait, see Figure 1) are rare, in part because of the hazard to equipment posed by intense fishing and trawling (Kawatate *et al.*, 1988). However, from many short-term measurements the general strength of the currents and the importance of tides have been demonstrated (Mizuno *et al.*, 1989; Egawa, 1993; Isobe *et al.*, 1994; Katoh *et al.*, 1996). Water masses in the Strait derive from the warm Tsushima Current as it flows from the East China Sea into the Japan/East Sea, although river runoff causes marked freshening near the Korean coast. Current direction is generally northeastward along the channel but southwestward countercurrents have been observed.

The Strait is the most important of the four straits that connect the Japan/East Sea with adjacent waters. It is the dominant inflow channel and determines the transfer of heat, salt, fish larvae, etc. into the Japan/East Sea. About 330 km long and 100 m deep, it has the form of a shallow channel connecting the broad East China Sea (depths of 50 m to 1000 m) and the much deeper (over 2000 m) Japan/East Sea. The narrows between Korea and Japan are 160 km wide and divided into two channels, East and West, by Tsushima Island. The Western Channel is distinguished by a closed topographic depression in its center that is approximately 60 km long, 10 km wide, and over 200 m deep at maximum. Its position is approximated in Figure 1 by the 150 m closed contour west and north of Tsushima Island.

Reported here are extensive current measurements made in the Strait as part of a multi-national effort to study the East Asian Marginal Seas. Six instrument packages were deployed along each of two lines (Figure 1) from May - October 1999. The southern line across the entrance to the Strait is defined by instrument sites S1 through S6; the northern line across its exit by N2 through N6. Site details are provided in Table 1.

2. Instruments and Methods

Each deployed package consisted of an acoustic Doppler current profiler (ADCP) and wave/tide gauge housed in a trawl-resistant bottom mount (TRBM). Nine of the deployments were based on a new type of TRBM known as Barny after its barnacle-like shape (Perkins *et al.*, 2000) and developed by SACLANT Center in Italy in collaboration with NRL. The remaining TRBMs, at sites N2, N3, and S5, were of a different design developed for the Naval Oceanographic Office (Teague *et al.*, 1998). The Barny mounts were equipped with RD Instruments Workhorse ADCPs operating at 300 KHz; those from NAVOCEANO with RD Instruments Narrowband ADCPs operating at 150 KHz. All packages contained Sea-Bird Electronics Model 26 wave/tide gauges and EdgeTech Model 8202 acoustic releases for location and recovery. The ADCPs were set up to provide current profiles with an accuracy of 1 cm/sec over nearly the full water column. Vertical resolution was set at 4 m, except 2 m at S1, S2 and N2.

Eleven of the moorings were recovered and redeployed along with two additional moorings during October, 1999. A

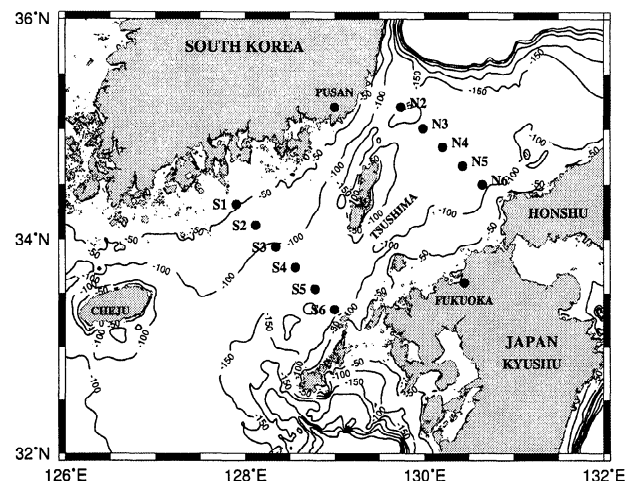


Figure 1. Mooring locations. Depth contours are based on the bathymetric database compiled by Dr. Byung-Ho Choi.

Copyright 2000 by the American Geophysical Union.

Paper number 2000GL011454.
0094-8276/00/2000GL011454\$05.00

Table 1. ADCP Summary. Depths and bin sizes are in m.

Site	Lat	Lon	Start Day	End Day	Top Bin	Bottom Bin	Bin Size	Water Depth
S1	34.32	127.90	130	289	5	53	2	59
S2	34.13	128.12	129	289	7	83	2	89
S3	33.93	128.34	129	288	11	103	4	113
S4	33.74	128.56	128	287	9	97	4	107
S5	33.54	128.78	128	287	19	143	4	152
S6	33.35	129.00	128	286	9	105	4	115
N2	35.20	129.67	125	282	25	137	2	142
N3	35.01	129.99	126	283	13	125	4	132
N4	34.84	130.21	126	283	13	117	4	127
N5	34.67	130.43	127	284	16	120	4	130
N6	34.50	130.65	127	284	12	108	4	118

twelfth instrument, located at a site (N1) between N2 and the Korean coast, could not be recovered, although it responded to acoustic interrogation. A visual and acoustic survey of the area using a remotely operated underwater vehicle revealed that the package had sunk into the bottom, which is very soft at that site.

We focus here on the subtidal portion of the current field. Profiles of vector velocity were recorded at either 15 min or 30 min intervals at each mooring. Tidal currents, which can exceed the mean, especially along the northern section, were thus well resolved. They have been removed in the results shown here by applying a low-pass filter with a 40-hour cutoff. Where appropriate, velocities are resolved into along- and across-section components, U and V . The rotations are 45° and 40° clockwise respectively for the south and north sections, so that U is positive southeastward and V positive northeastward.

3. Observations

Time-mean current vectors at all sites and various depths are shown in Figure 2, and statistics for the cross-section (V) component of vertically-averaged velocities in Table 2. Discussion in the following two paragraphs, one for each section, is based on this Figure and Table plus more extensive displays not shown here.

Along the southern section, V varies smoothly between S1 and S6, with a broad maximum at mid-channel. Currents at S2 through S6 are predominantly across-section and are only weakly depth dependent, except that at S6 they are much reduced near the bottom. At S1, the flow is predominantly northward, being almost directly northward near the surface and bottom. At all sites V is positive (towards 045°) and is much larger than the standard deviation except at the two end stations. Nevertheless, strong tidal and non-tidal currents towards the southwest are common. These sporadic countercurrents occur throughout the water column, most notably at S1, S5, and S6.

A countercurrent along the southeastern end of the section has also been observed by Katoh, et al. (1996) using a ship mounted ADCP. Along-section mean currents (U) are southeast at 10 cm/s or less, except at S1. Strongest northwestward mean flows (negative U) are found at S1 and at S3; those at the latter site are due to northward veering near the bottom. Typhoons near days 02 August and 22 September were not accompanied by strong current anomalies.

The northern section shows strong site-to-site variability. Strong mean northeastward flow occurs at N2, N5 and N6, while the mid-channel sites N3 and N4 are conspicuously weaker than their neighbors. Along-section currents are weak at N5 and N6. Currents at N2 vary smoothly with depth from 35° east of north near the surface, approximately parallel to the coast and local bathymetric contours, to 35° west of north near the bottom (Figure 2). This bottom current at N2 is directed strongly shoreward at 20 cm/s in the mean and at over 30 cm/s during the first half of the recording period.

Figure 3 displays mean currents and deviation ellipses at three depth levels and as a vertical average. There is a 63 % probability that the mean vector lies within its deviation ellipse, assuming a bivariate Gaussian distribution (Perkins et al., 1998). The strongest currents have means much larger than their respective deviation ellipses. In this sense, the best determined depth-averaged currents are at S3 and N6. Overall maximum mean current velocities are observed at S3 during September - October. Indeterminate mean currents are found nearest the coasts on the southern line (S1, S6) and at mid-channel on the northern line (N3, N4) where the mean vectors

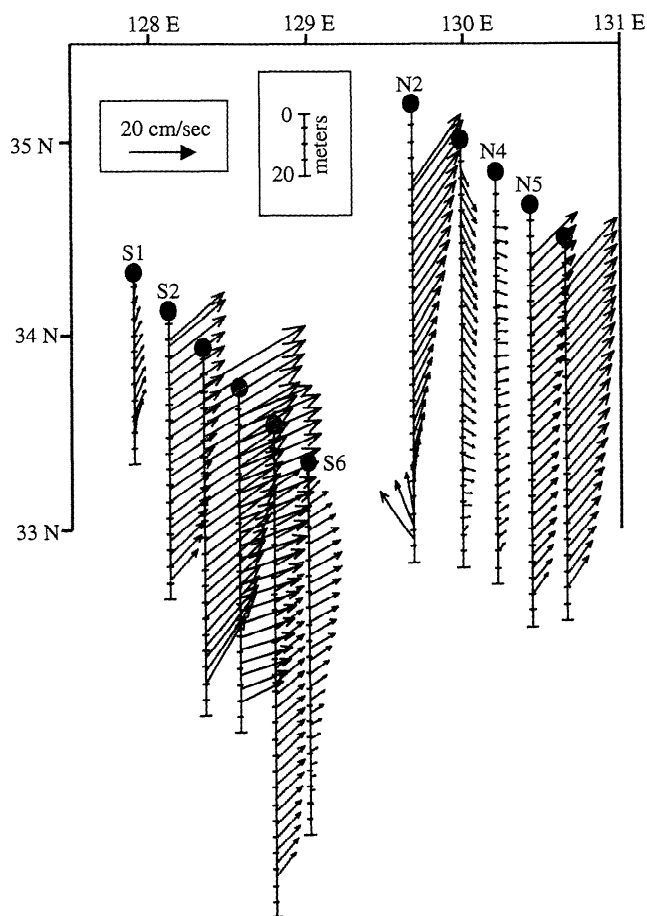


Figure 2. Time-averaged velocity vectors for all sites and all depths. Mooring locations are marked by a red circle referenced to the geographical coordinates. A vertical line extending downward from the symbol denotes depth from surface to bottom. Individual vectors are drawn in plan view, as though the surface of the page were a horizontal plane, with the vector originating from its respective depth on the vertical line. Thus, the uppermost current vector at site N2 is at about 25 m depth and directed towards the northeast.

Table 2. Statistics for velocity component normal to the section. \underline{V} is the mean over time and depth and $\sigma\underline{V}$ is the standard deviation around it of the de-tided signal. Minima and maxima of vertically averaged de-tided currents are denoted by \underline{V}_{\min} and \underline{V}_{\max} . Minima and maxima for total current (without tide removal or depth averaging) are Vt_{\min} and Vt_{\max} .

Site	\underline{V}	$\sigma\underline{V}$	\underline{V}_{\min}	\underline{V}_{\max}	Vt_{\min}	Vt_{\max}
S1	5.4	7.2	-25.7	32.0	-93.6	122.8
S2	17.8	8.0	-18.5	34.6	-71.2	125.6
S3	29.5	6.1	12.6	48.1	-53.1	123.4
S4	21.5	5.8	8.6	46.9	-73.7	123.2
S5	11.2	4.3	-2.5	24.4	-71.3	92.4
S6	7.3	6.1	-7.2	28.1	-85.7	97.5
N2	17.5	9.9	-6.6	52.4	-84.7	130.7
N3	-1.3	6.3	-18.5	20.2	-97.5	95.6
N4	2.2	6.1	-19.7	19.1	-84.6	73.2
N5	14.0	6.6	-2.3	35.6	-60.4	116.6
N6	20.4	6.1	2.5	35.8	-68.9	106.0

are entirely contained within their deviation ellipses. Variability is greatest during September - October and smallest during May - June. Mean direction is fairly consistent between these two time periods, except at N3 and N4. Monthly mean directions near the bottom are similar over the entire recording period. At the two sites nearest the Korean coast (S1, N2), near-bottom currents flow persistently toward the coast.

In Figure 4, across-section velocities are displayed as two-dimensional fields of de-tided currents at a few representative

times. In these snapshots, currents have been extrapolated to the coasts by assuming them constant along horizontal lines. The southern section (Figure 4a-d) shows a high velocity core with velocities of 30 cm/s and greater over the region of uniform bottom slope. Strong currents with high variability, including occasional flow reversals, are found near the Japanese coast on the southern line, although the reversals do not extend to the surface. At the other end of the section, near the Korean coast, the strong counterflow at S1 on September 18 (panel d) corresponds to Vt_{\min} in Table 2.

Representative snapshots for the northern line are shown in Figure 4e-h. As noted earlier, strongest northeastward-directed currents are frequently found near extremities of the section, near the coasts of Korea and Japan. They can extend from the surface to bottom or can form a subsurface jet. Currents near midsection often feature a counter flow towards the southwest, sometimes extending from surface to bottom. A sporadic, deep counter current is found in the depression at the Korean end of the section. It is associated with the movement of cold water into the Strait from the Japan/East Sea (Lim, 1973) and is sometimes accompanied by a strong northeastward surface flow (Isobe, 1995).

Transport through the southern section, where the current structure makes it straightforward to estimate, is approximately 3.3 Sv, with little month-to-month variation during these measurements. A detailed treatment of transport is in progress.

4. Discussion

The single core of current apparent in our southern section separates into two branches before reaching the northern

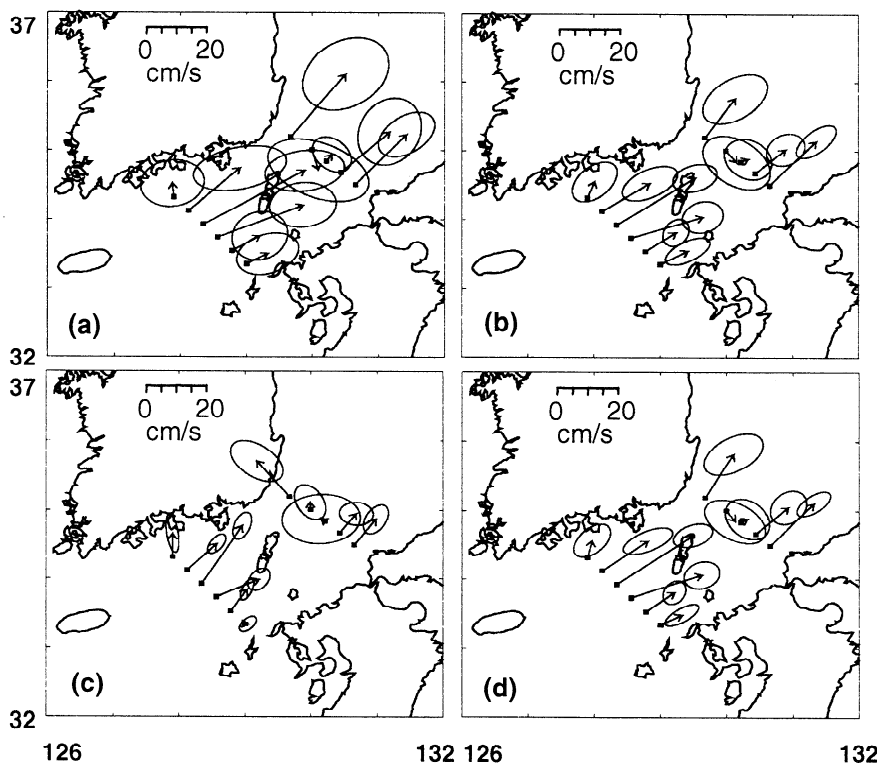


Figure 3. Mean current vectors: (a) near the surface (shallowest ADCP depth bin), (b) at mid-depth (middle bin), (c) near the bottom (deepest bin), and (d) depth-averaged. Means and deviations are based on de-tided currents over the full May - October observing period.

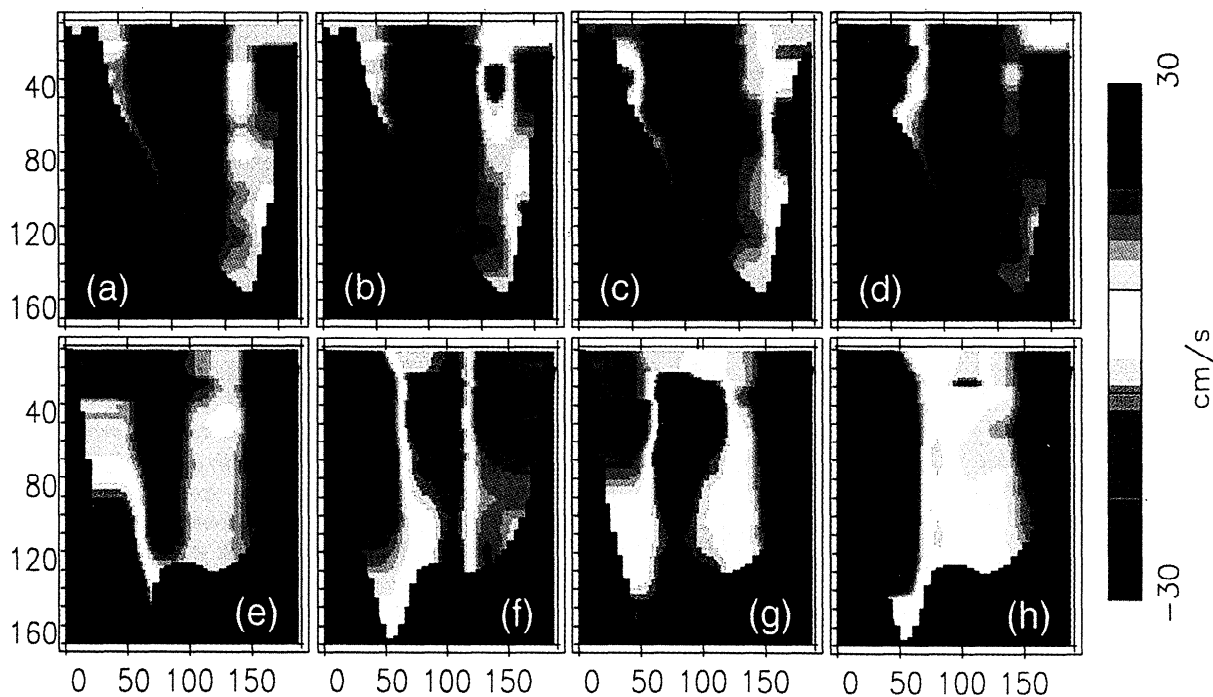


Figure 4. Snapshots of velocities for representative current patterns for the south (a-d) and north (e-h) sections after tide removal. Horizontal axes are in km; vertical axes are in m.

section. The two branches are separated by a region (sites N3 and N4) where currents are variable and lack a well-defined mean. It is difficult to escape the conclusion that the single current core found upstream is divided by its passage around Tsushima Island, and that the band of variability is an island-induced wake. It is well established that flow from the Strait takes two divergent paths in the Japan/East Sea. One branch, the East Korean Warm Current, flows northward along the eastern coast of Korea; the other flows eastward along the northern coast of Japan. However, the bifurcation point is not well established (Kaneko *et al.*, 1991; Katoh *et al.*, 1996). We presume that the two streams apparent in our northern mooring line are an expression of this separation. Subsequent exchange between these branches further downstream is constrained by nearness of deep waters of the Japan/East Sea (it is less than 50 km from site N2 to the 1000 m isobath) where the constraint to follow bathymetric contours can play a dominant role.

Acknowledgments. This work was supported by the Office of Naval Research as part of the Basic Research Project "Dynamical Linkage of the Asian Marginal Seas" under Program Element PE0601153N (NRL-SSC contribution 7332--00-0009).

References

- Egawa, T., Y. Nagata, and S. Sato, Seasonal variation of the Current in the Tsushima Strait deduced from ADCP data of ship-of-opportunity, *J. Ocean.*, **49**, 39-50, 1993.
- Isobe, A., S. Tawara, A. Kaneko, and M. Kawano, Seasonal variability in the Tsushima Warm Current, Tsushima-Korea Strait, *Cont. Shelf Res.*, **14**, 23-35, 1994.
- Isobe, A., The influence of the bottom cold water on the seasonal variability of the Tsushima Warm Current, *Cont. Shelf Res.*, **15**, 763-777, 1995.
- Katoh, O., K. Teshima, K. Kubota, and K. Tsukiyama, Downstream transition of the Tsushima Current west of Kyushu in summer, *J. Ocean.*, **52**, 93-108, 1996.
- Kaneko, A., S.-K. Byun, S.-D. Chang, and M. Takahashi, An observation of sectional velocity structures and transport of the Tsushima Current across the Korea Strait, in *Oceanography of Asian Marginal Seas*, edited by K. Takano, pp.179-195, Elsevier, Amsterdam, 1991.
- Kawatate, K., T. Miita, Y. Ouchi, and S. Mizuno, A report on failures of current meter moorings set east of Tsushima Island from 1983 to 1987, *Prog. Oceanogr.*, **21**, 319-327, 1988.
- Lim, D. B., The movement of the cold water in the Korea Strait, *J. Oceanol. Soc. of Korea*, **8**, 46-52, 1973.
- Mizuno, S., K. Kawatate, T. Nagahama, and T. Miita, Measurements of East Tsushima Current in winter and estimation of its seasonal variability, *J. Oceanogr. Soc. Japan*, **45**, 375-384, 1989.
- Perkins, H., T. S. Hopkins, S.-A. Malmberg, P. Poulain, and A. Warn-Varnas, Oceanographic conditions east of Iceland, *J. Geophys. Res.*, **103**, 21,531-21,542, 1998.
- Perkins, H., F. de Strobel, and L. Gualdesi, The Barny Sentinel Trawl-resistant ADCP bottom mount: design, testing, and application, *IEEE J. Oceanic Eng.*, October, 2000 (accepted).
- Teague, W. J., H. T. Perkins, Z. R. Hallock, and G. A. Jacobs, Current and tide observations in the southern Yellow Sea, *J. Geophys. Res.*, **103**, 27,783-27,793, 1998.
- G. A. Jacobs, H. Perkins, and W. J. Teague, Naval Research Laboratory, Stennis Space Center, MS 39529. (e-mail: hperkins, teague, or jacobs@nrlssc.navy.mil)
- K. I. Chang and M. S. Suk, Korea Ocean Research and Development Institute, Ansan, P. O. Box 29, Seoul 425-600, Korea. (e-mail: kichang or mssuk@kordi.re.kr)

(Received: January 28, 2000; Accepted: July 19, 2000.)